# Computer Simulation of Phenyl Ester Cleavage by β-Cyclodextrin in Solution

**Victor Luzhkov*,† and Johan Åqvist*,‡**

*Contribution from the Institute of Chemical Physics in Chernogolovka, Russian Academy of Sciences, Chernogolovka, Moscow Region, 142432, Russia, and Department of Molecular Biology, Uppsala Biomedical Center, Box 590, S-75124 Uppsala, Sweden*

*Received November 4, 1997. Revised Manuscript Received April 13, 1998*

**Abstract:** Molecular dynamics free energy perturbation simulations utilizing the empirical valence bond model are used to study the catalytic action of β-cyclodextrin in ester hydrolysis. Reaction routes for nucleophilic attack on *m-tert*-butylphenyl acetate by the secondary alkoxide ions O2$^-$ and O3$^-$ of cyclodextrin giving the *R* and *S* stereoisomers of the ester tetrahedral intermediate are examined. Only the reaction path leading to the *S* isomer at O2 shows an activation barrier that is lower (by about 3 kcal/mol) than the barrier for the corresponding reference reaction in water. The calculated rate acceleration is in excellent agreement with experimental data. The catalytic action is accompanied by distortion of the macrocycle structure that enables strong binding of the nonpolar part of the substrate along most of the reaction path.

## Introduction

Studies of organic catalysts that can mimic the reactivity of enzyme systems are one of the exciting challenges of modern chemistry. The possibility of theoretical examination of these types of problems on a detailed microscopic level has been greatly enhanced during the past years owing to the development of powerful computational techniques. Modern theoretical methods allow the characterization of various aspects of biomimetic chemical reactivity. Most simulations of thermodynamic and kinetic properties of solvated biomimetic systems are performed by means of statistical physical methods such as molecular dynamics (MD) and Monte Carlo. These methods usually involve treating intra- and intermolecular interactions by force field (FF) representations. The nature of FF's generally does not allow the calculation of energetics associated with changes in bonding pattern during chemical reactions. A rigorous treatment of electronic effects on the potential surfaces along reaction paths can be performed with high end quantum chemical ab initio methods, but their use is currently technically feasible only for a small subspace of the catalytic site. One way of treating chemical reactions in solution and enzymes in a more realistic manner is provided by the empirical valence bond (EVB) free energy perturbation (FEP) approach.[1−3] The MD/FEP/EVB method combines the treatment of different states along a chemical reaction path in terms of valence bond configurations with extensive molecular dynamics sampling and the computational efficiency of empirical force fields, and this method has been successfully employed in molecular modeling of several types of enzyme reactions.[1−3]

Cyclodextrins have attracted a long-standing interest in the field of artificial catalysts.[4−7] These cone-shaped macrocycles are composed of α,D-glucose subunits and possess a nonpolar cavity with hydrophilic rims containing primary and secondary hydroxyl groups. Cyclodextrins form inclusion complexes with a variety of polar and nonpolar compounds and are widely used in chromatography to separate stereoisomers. They serve as templates in supramolecular design and for some special substrates mimic the action of hydrolytic proteins, such as chymotrypsin. In reactions with aromatic esters cyclodextrins accelerate the rate of their hydrolysis in a way that is consistent with enzyme action in that it involves both a stage of preliminary binding and subsequent reaction in the specifically arranged complex.[4−6,8] Structural properties of cyclodextrin molecules in the gas phase, in crystals, and in the presence of solvent have been studied with force field methods.[9−11] Binding of different guests to cyclodextrins has also been the subject of a number of computer simulations.[10,12,13] Furthermore, inclusion complexes of cyclodextrins with aromatic esters formed in the primary stage of hydrolysis have been studied with molecular

† Russian Academy of Sciences.

‡ Uppsala Biomedical Center.

(1) (a) Warshel, A.; Weiss, R. M. *J. Am. Chem. Soc*. **1980**, *102*, 6218. (b) Warshel, A.; Russel, S. J. *J. Am. Chem. Soc*. **1986**, *108*, 6569. (c) Hwang, J.-K.; King, G.; Creighton, S.; Warshel, A. *J. Am. Chem. Soc*. **1988**, *110*, 5297. (d) Warshel, A.; Sussman, F.; Hwang, J.-K. *J. Mol. Biol*. **1988**, *201*, 139. (e) Åqvist, J.; Warshel, A. *Biochemistry* **1989**, *28*, 4680.

(2) Warshel, A. *Computer Modeling of Chemical Reactions in Enzymes and Solutions*; John Wiley & Sons: New York, 1991.

(3) (a) Åqvist, J.; Warshel, A. *Chem. Rev*. **1993**, *93*, 2523. (b) Schweins, T.; Langen, R.; Warshel, A. *Nature Struct. Biol.* **1994**, *1*, 476. (c) Åqvist, J.; Fothergill, M. *J. Biol. Chem.* **1996**, *271*, 10010. (d) Åqvist, J. In *Computational Approaches to Biochemical Reactivity*; Naray-Szabo, G., Warshel, A., Eds.; Kluwer: Dordrecht, The Netherlands, 1997; pp 341−362.

(4) (a) Bender, M. L.; Komiyama, M. *Cyclodextrin Chemistry*; Springer-Verlag: Berlin, 1978. (b) Bender, M. L.; Bergeron, R. J.; Komiyama, M. *The Bioorganic Chemistry of Enzymatic Catalysis*; John Wiley & Sons: New York, 1984; pp 265−305.

(5) (a) Breslow, R. *Adv. Chem. Ser*. **1980**, *191*, 1. (b) Breslow, R. *Science* **1982**, *218*, 532.

(6) (a) Saenger, W. *Angew. Chem., Int. Ed. Engl.* **1980**, *19*, 344. (b) Szejtli, J. *Cyclodextrins and their Inclusion Complexes*; Akademiai Kiado: Budapest, 1982.

(7) (a) Szejtli, J. *Cyclodextrin Technology*; Kluwer: Dordrecht, The Netherlands, 1988. (b) *Biotechnology of Amylodextrin Oligosaccharides*; Friedman, R. B., Ed.; ACS Symp. Ser. No. 458; American Chemical Society: Washington, DC, 1991.

(8) (a) VanEtten, R. L.; Sebastian, J. F.; Clowes, G. A.; Bender, M. L. *J. Am. Chem. Soc*. **1967**, *89*, 3242. (b) VanEtten, R. L.; Sebastian, J. F.; Clowes, G. A.; Bender, M. L. *J. Am. Chem. Soc*. **1967**, *89*, 3253. (c) Breslow, R.; Czarniecki, M. F.; Emert, J.; Hamaguchi, H. *J. Am. Chem. Soc*. **1980**, *102*, 762.

S0002-7863(97)03799-2 CCC: $15.00 
Published on Web 06/05/1998

mechanics.[14] Semiempirical quantum chemical calculations have been performed in studies of solvent effects on hydrolysis[15] and decarboxylation[16] reactions accelerated by cyclodextrins. The calculations of ref 15, where solvent was modeled by the Langevin Dipole (LD) model,[2] provided an important insight into the role of the macrocycle cavity in catalysis and also pointed to the necessity of including thermal conformational sampling in modeling structural reorganization of cyclodextrin along the hydrolysis reaction path.

In this paper we employ the MD/FEP/EVB technique for studying ester cleavage in *m*-*tert*-butylphenyl acetate (*mt*BPA) in reaction with $\beta$-cyclodextrin ($\beta$CD), where $\beta$-cyclodextrin is a macrocycle composed of seven α-1,4-linked D-glucose units (Figure 1). The first rate limiting stage of this reaction, namely formation of the tetrahedral intermediate (TI) at the acyl carbon atom, is considered in this work (Scheme 1). The *mt*BPA substrate is chosen because of a marked increase (up to a factor of 250) of the reaction rate compared to hydrolysis in water by hydroxide ion, glucoside, or glucose molecules.[8a] Accordingly, our study evaluates reaction free energy profiles for ester hydrolysis in two cases, which are identical with regard to the structure of the reaction center but proceed in different microenvironments. The reference reaction 1 involves nucleophilic attack of alkoxide ion from α-methyl glucoside at the acyl carbon of phenyl acetate in water, while the catalyzed reaction 2 takes place in the cyclodextrin cavity with the participation of one of seven equivalent glucose units. The reactivity of alkoxide ions derived from the C2 and C3 secondary hydroxyl groups (−O2−H and −O3−H) of the glucose unit is studied in both cases.

## Methods

The FEP/EVB method is a powerful approach for investigation of reaction free energy surfaces. The method has been discussed in detail in refs 1−3, so here we will only provide a short description of the main steps involved in setting up the simulations. In our treatment, reactions 1 and 2 (Scheme 1) are considered as an effective two-state problem corresponding to the valence bond structures

$$\phi_1 = (\mathrm{C{=}O})(\mathrm{O}^-)$$

$$\phi_2 = (\mathrm{O{-}C{-}O}^-) \qquad (3)$$

where C═O, $O^-$, and $O-C-O^-$ indicate the carbonyl group of phenyl acetate, the alkoxide ion of methyl glucoside (or a glucose residue of $\beta$CD), and the tetrahedral intermediate, respectively. The energies of the two diabatic states (eq 3) are described in terms of analytical potential energy functions and written as

$$\epsilon_i = H_{ii} = \sum_j \Delta M_j^{(i)}(b_j^{(i)}) + \frac{1}{2}\sum_l \gamma_l^{(i)} k_l^{(i)}(\theta_l^{(i)} - \theta_{0,l}^{(i)}) + \frac{1}{2}\sum_m \gamma_m^{(i)} K_m^{(i)} \times [1 + \cos(n_m^{(i)} \phi_m^{(i)} - \delta_m^{(i)})] + V_{nb,rr}^{(i)} + \alpha^{(i)} + V_{nb,rs}^{(i)} + V_{ss} \quad (4)$$

Here, all the energy terms except the last one ($V_{ss}$) represent interactions involving the reacting fragments, and these terms thus usually look different for different bonding configurations (the subscript *r* is used to denote the reacting fragments, while *s* denotes their surroundings). The first three terms in eq 4 are those for bonds (Morse potentials)

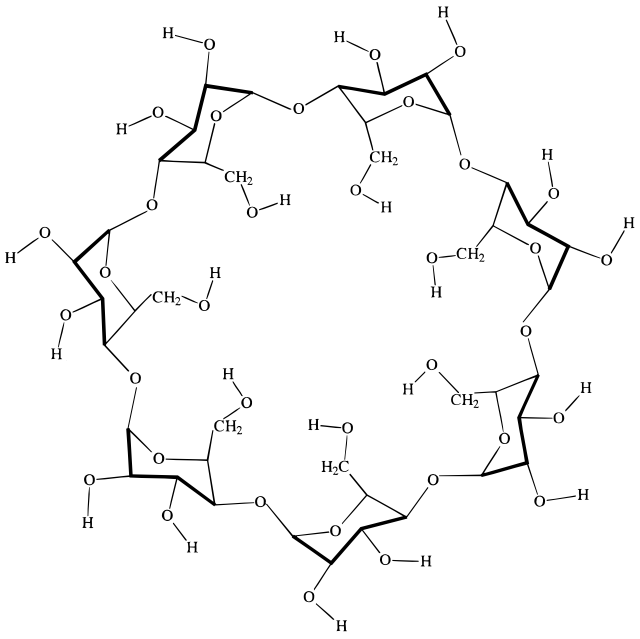

**Figure 1.** Schematic structure of $\beta$-cyclodextrin with primary and secondary hydroxyls. The broader rim of the macrocycle cavity is presented with solid lines.

**Scheme 1**

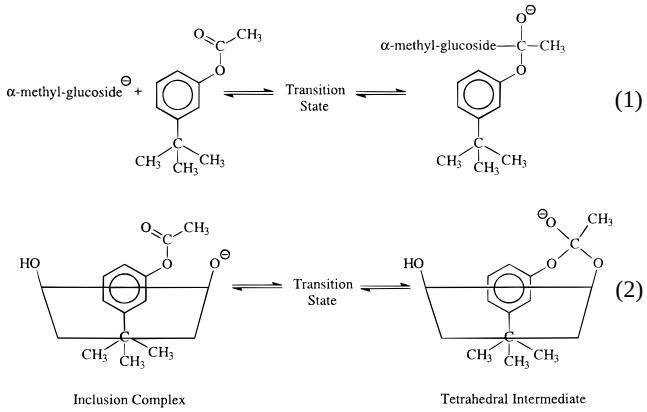


(9) (a) Koehler, J. E. H.; Saenger, W.; van Gunsteren, W. F. *Eur. J. Biophys.* **1987**, *15*, 197. (b) Koehler, J. E. H.; Saenger, W.; van Gunsteren, W. F. *Eur. J. Biophys.* **1987**, *15*, 211. (c) Koehler, J. E. H.; Saenger, W.; van Gunsteren, W. F. *Eur. J. Biophys.* **1988**, *16*, 153. (d) Koehler, J. E. H. In *Molecular Dynamics: Application in Molecular Biology*; Goodefellow, J. M. D., Ed.; CRC: Boca Raton, FL, 1990; pp 69−106. (e) Venanzi, C. A.; Canzius, P. M.; Zhang, Z.; Bunce, J. D. *J. Comput. Chem.* **1989**, *10*, 1038. (f) Wertz, D. A.; Shi, C. X.; Venanzi, C. A. *J. Comput. Chem.* **1992**, *13*, 41. (g) Immel, S.; Brickmann, J.; Lichtenthaler, F. W. *Liebigs Ann.* **1995**, *6*, 929.

(10) Lipkowitz, K. B.; Green, K.; Yang, J.-A. *Chirality* **1992**, *4*, 205.

(11) (a) Koehler, J. E. H.; Saenger, W.; van Gunsteren, W. F. *J. Mol. Biol.* **1988**, *203*, 241. (b) Linert, W.; Margl, P.; Renz, F. *Chem. Phys.* **1992,** *161*, 327. (c) Berthault, P.; Duchesne, D.; Desvaux, H.; Gilquin, B. *Carbohydr. Res.* **1995**, *276*, 267.

(12) (a) Kostense, A. S.; van Helden, S. P.; Janssen, L. H. *J. Comput. Aided Mol. Des.* **1991**, *5*, 225. (b) van Helden, S. P.; van Eijck, B. P.; Janssen, L. H. *J. Biomol. Struct. Dyn.* **1992**, *9*, 1269. (c) Ohashi, M.; Kasatani, K.; Shinohara, H.; Sato. H. *J. Am. Chem. Soc.* **1990**, *112*, 5824. (d) Lipkowitz, K. B.; Raghothama, S.; Yang, J. *J. Am. Chem. Soc.* **1992**, *114*, 1554. (e) Koehler, J. E. H.; Manfred, H.; Richters, M.; Konig, W. A. *Angew. Chem., Int. Ed. Engl.* **1992**, *3*, 319. (f) Durham, D. G.; Liang, H. *Chirality* **1994**, *6*, 239. (g) Kohler, J. E. H.; Hohla, M.; Richters, M.; Konig, W. A. *Chem. Ber.* **1994**, *127*, 119.

(13) (a) Tesarova, E.; Gilar, M.; Hobza, P.; Kabelac, M.; Deyl, Z.; Smolkovakeulemansova, E. *HRC-J. High Res. Chromatogr.* **1995**, *18*, 597. (b) Klein, C. T.; Kohler, G.; Mayer, B.; Mraz, K.; Reiter, S.; Viernstein, H.; Wolschann, P. J. *Inclusion Phenom. Mol. Recogn.* **1995**, *22*, 15. (c) Black, D. R.; Parker, C. G.; Zimmerman, S. S.; Lee, M. L. *J. Comput. Chem.* **1996**, *17*, 931. (d) Ivanov, P. M.; Jaime, C. *J. Mol. Struct.* **1996**, *377*, 137. (e) Lichtenthaler, F. W.; Immel, S. *Liebigs Ann.* **1996**, *1*, 27. (f) Jursic, B. S.; Zdravkovski, Z.; French, A. D. *J. Mol. Struct. (THEOCHEM)* **1996**, *366*, 113. (g) Manunza, B.; Deiana, S.; Pintore, M.; Delogu, G.; Gessa, C. *Carbohyd. Res.* **1997**, *300*, 89.

(14) (a) Menger, F. M.; Sherrod, M. J. *J. Am. Chem. Soc.* **1988**, *110*, 8606. (b) Thiem, H.-J.; Brandl, M.; Breslow, R. *J. Am. Chem. Soc.* **1988**, *110*, 8612.

(15) Luzhkov, V. B.; Venanzi, C. A. *J. Phys. Chem.* **1995**, *99*, 2312.

(16) Furuki, T.; Hosokawa, F.; Sakurai, M.; Inoue, Y.; Chujo, R. *J. Am. Chem. Soc.* **1993**, *115*, 2903.

and bond angles and torsional angles (including improper ones) that involve the reacting fragments. Bond angle and torsional energies can also depend on the degree of formation of certains bonds through the coupling factor $\gamma_l^{(i)} = |M_j^{(i)}/D_j^{(i)}|$, where $D_j^{(i)}$ is the dissociation energy of the particular bond ($j$) to which the $l$th angle or torsion is coupled.[3d] $V_{nb,rr}$ and $V_{nb,rs}$ are the nonbonded electrostatic and van der Waals (Lennard-Jones) interactions among the reacting atoms themselves and with the surrounding atoms, respectively. These terms will, of course, differ between resonance structures as the charges and Lennard-Jones parameters can change between the VB states. The last term in eq 4 is the "invariant" part pertaining to interactions involving only the surrounding atoms, i.e., harmonic bond and angle terms, proper and improper torsions, and electrostatic and Lennard-Jones terms. While standard force fields can describe the interactions between the fragments in each state and with the surrounding medium, as well as the energies associated with distorting geometries away from their equilibrium, they do not provide information regarding absolute or even relative energies of the reacting fragments in a vacuum when they are noninteracting and at their equilibrium geometries. There is thus a real energy difference between the resonance structures determined by their heats (or free energies) of formation in the gas phase that is usually not given by molecular mechanics FF's. This is reflected by the constants $\alpha^{(i)}$, which will enter as the difference, $\Delta\alpha = \alpha^{(2)} - \alpha^{(1)}$, in the energy between $\phi_1$ and $\phi_2$ with the reacting fragments at infinite separation in the gas phase. This quantity can thus be obtained either from gas-phase experimental data or ab initio calculations or by calibration of simulated and observed reaction profiles for suitable reference reactions in water.[1−3] This latter alternative has proven to be particularly useful and will be adopted here also.

The ground-state energy of the system is calculated at any configuration from the solution of the 2 × 2 secular equation,

$$E_g = {}^1/_2(\epsilon_1 + \epsilon_2) - {}^1/_2[(\epsilon_1 - \epsilon_2)^2 + 4H_{12}^2]^{1/2}$$

where $H_{12}$ is the off-diagonal Hamiltonian matrix element that mixes the two diabatic surfaces. In most earlier EVB studies it has been represented by an exponential function

$$H_{12} = A_{12}\exp(-\mu_{12}r_{XY})$$

of the distance between two atoms, or simply by a constant value.[1−3] In this work we will also consider the approach outlined by Chang and Miller,[17] who derive a generalized Gaussian form for the exchange matrix element. The off-diagonal function is then represented by

$$H_{12} = A_{12}\exp[\mu_{12}(r_{XY} - r_{XY}^{\ddagger}) - \eta_{12}(r_{XY} - r_{XY}^{\ddagger})^2] \qquad (5)$$

where $r_{XY}$ in our case denotes the distance between the two atoms (O and C) forming the new bond and $r_{XY}^{\ddagger}$ is the corresponding value of this distance in the transition state region.

The calculations of free energy profiles follow the FEP procedure described in refs 1−3. The two VB states are "connected" via a set of intermediate mapping potentials $\epsilon_m = \lambda_1^m\epsilon_1 + \lambda_2^m\epsilon_2$, where $\lambda_1^m + \lambda_2^m = 1$. The mapping vector $\vec{\lambda}_m = (\lambda_1^m,\lambda_2^m)$ changes between the values (1,0) of reactants and (0,1) of products. The free energy associated with changing $\epsilon_1$ to $\epsilon_2$ in $n$ discrete steps is obtained as

$$\Delta G(\vec{\lambda}_n) = \Delta G(\vec{\lambda}_0 \rightarrow \vec{\lambda}_n) = -RT\sum_{m=0}^{m=n-1} \ln\langle\exp[-(\epsilon_m - \epsilon_m)/\mathrm{RT}]\rangle_m \qquad (6)$$

where the average $\langle\ \rangle_m$ is evaluated on the potential surface $\epsilon_m$. The free energy, $\Delta G(X^n)$, corresponding to the trajectories moving on the actual ground-state potential, $E_g(X^n)$, is calculated from the umbrella sampling expression

$$\Delta G(X^n) = \frac{\sum_{m\supset\Delta\epsilon=X^n} w_m[\Delta G(\vec{\lambda}_m) - RT\ln\langle\exp\{-[E_g(X^n) - \epsilon_m(X^n)]/RT\}\rangle_m]}{\sum_{m\supset\Delta\epsilon=X^n} w_m} \qquad (7)$$

where the discretized reaction coordinate $X^n$ is defined in terms of the energy gap $\Delta\epsilon = \epsilon_1 - \epsilon_2$, between the two diabatic surfaces. The sums in eq 7 run over those $m$ for which the mapping vector $\vec{\lambda}_m$ samples the reaction coordinate interval $X^n$, i.e., those containing configurations with $\Delta\epsilon = X^n$, and their weights ($w_m$) are given by the number of such configurations. In calibration of the uncatalyzed reaction surface, $\Delta G(X^n)$ is used iteratively to determine the parameters $\Delta\alpha$ and $H_{12}$ so that the calculated and experimental values of reaction free energies and activation barriers coincide.

The GROMOS force field[18a] with minor revisions[18b] is employed in the present calculations and bond and angle parameters calibrated for cyclodextrins are taken from ref 9a. Other relevant parameters used in the calculations are listed in Table 1. Atomic charges for the reaction species of Scheme 1 are given in Figure 2, and most charges correspond to the standard GROMOS values. Exceptions are the acyl carbon atom and atoms of the reactive center of the tetrahedral intermediate. Such atom types are not present in the standard GROMOS charge set and the corresponding charges have been fitted to preserve the total charge of the relevant fragments. The charges on the acyl carbon atom and methyl group in the tetrahedral intermediate are changed by 0.1$e$ compared to the charges of neutral phenyl acetate (according to earlier AM1 calculations).[15] In the EVB treatment the parameters describing the reaction surface of a reference reaction are calibrated by using available experimental data on hydrolysis in polar media. The free energy $\Delta G_{ref}^0$ of the aqueous reference reaction 1 is estimated to be +5 kcal/mol (see refs 1 and 19), while the observed reaction rate for attack by α-methyl glucoside in water corresponds to an activation energy, $\Delta G_{ref}^{\ddagger}$, of 21.8 kcal/mol.[8a] The parameters $\Delta\alpha$ and $H_{12}$ were thus adjusted to fit the calculated values of $\Delta G_{ref}^0$ and $\Delta G_{ref}^{\ddagger}$ of reaction 1 to the given experimental energies. This was done separately for the reactions at O2 and O3 as is discussed below.

In Table 1 we list the values of $\Delta\alpha$, $A_{12}$, and $\eta_{12}$ that reproduce the energetics of the reference reactions with methyl glucoside when $\mu_{12} \equiv 0$ (Gaussian form of $H_{12}$) and $r_{CO}^{\ddagger}$ is set to 2.0 Å. It turns out that, provided that the calculated $\Delta G_{ref}^0$ and $\Delta G_{ref}^{\ddagger}$ (of the uncatalyzed reactions at O2 and O3) are exactly calibrated to their target values, the resulting free energy profiles are remarkably insensitive to the form chosen for $H_{12}$. For instance, a change of $r_{CO}^{\ddagger}$ to 2.2 Å yields slightly different calibration values of $\Delta\alpha$, $A_{12}$, and $\eta_{12}$, but the resulting free energy profiles for both the (calibrated) uncatalyzed reference reactions 1 and the (predicted) βCD-catalyzed reactions remain virtually identical to those obtained with $r_{CO}^{\ddagger} = 2.0$ Å. Even calibration with a constant $H_{12}$ ($A_{12} = 68.8$, $\Delta\alpha = 47.2$ kcal/mol for the O2 reaction) produces identical free energy profiles, which clearly demonstrates the robustness of the EVB model. That is, the *difference* between the free energy surfaces in water and in βCD shows no appreciable dependence on the choice of form for the exchange matrix element, and all of the above calibrations even yield the same transition state geometry (see below). As said above, $\Delta\alpha$ refelects the energy difference between the isolated VB states in the gas phase. The reason why this quantity is positive is that there are fairly large intrinsic negative energy contributions in the gas phase TI due to internal H-bonding as well as the nonbonded exclusion logic of the FF. The difference in $\Delta\alpha$ between the Gaussian and constant $H_{12}$ also reflects a larger relative (more negative) effect of the former on the TI energy compared to the reactants. The overall energetics implied by the EVB calibrations for the gas-phase reference (methyl glucoside) reaction is still exothermic, in agreement with ab

(17) Chang, Y.-T.; Miller, W. H. *J. Phys. Chem.* **1990**, *94*, 5884.

(18) (a) van Gunsteren, W. F.; Berendsen, H. J. C. *Groningen Molecular Simulation (GROMOS) Library Manual*; Biomos B.V.: Nijenborgh 16, Groningen, The Netherlands, 1987. (b) Åqvist, J.; Medina, C.; Samuelsson, J.-E. *Protein Eng.* **1994**, *7*, 385. (c) Ryckaert, J. P.; Cicotti, G.; Berendsen, H. J. C. *J. Comput. Phys.* **1977**, *23*, 327.

**Table 1.** Parameters Used in the Calculations (in kcal/mol and Å)

| | |
|---|---|
| Morse<br>C−O ($\phi_2$) | $\Delta M(b) = D_M(1 - \exp(-\mu(b - b_0))^2$<br>$D_M = 84.00$, $b_0 = 1.43$, $\mu = 2.00$ |
| repulsive<br>C···O ($\phi_1$) | $V_{rep} = C_{ij}e^{-ar}$<br>$C_{ij} = 71.00$, $a = 1.58$ |
| EVB parameters,<br>reaction at O2 | $A_{12} = 60.5$, $\mu_{12} = 0$, $\eta_{12} = 0.14$, $r^{\ddagger}_{XY} = 2.0$<br>$\Delta\alpha = 61.7$ |
| EVB parameters,<br>reaction at O3 | $A_{12} = 53.7$, $\mu_{12} = 0$, $\eta_{12} = 0.14$, $r^{\ddagger}_{XY} = 2.0$<br>$\Delta\alpha = 43.0$ |

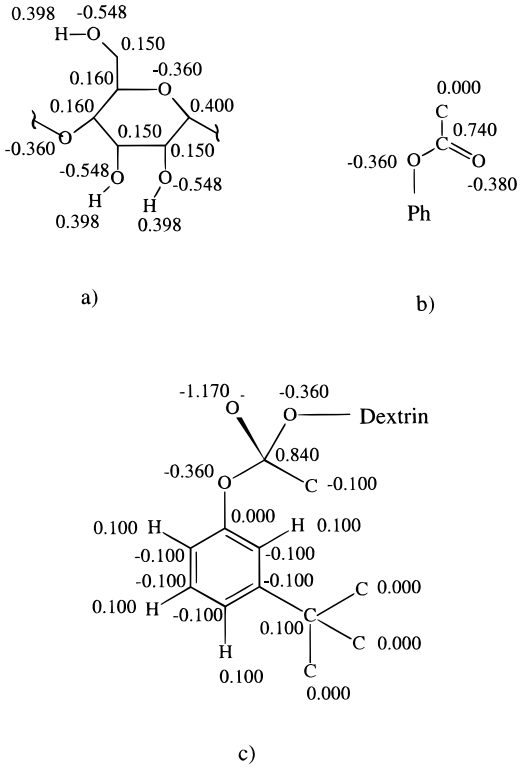


**Figure 2.** Atomic charges used with the GROMOS force field:[18a] (a) α,D-glucose subunit in $\beta$CD, (b) acyl group in *mt*BPA, and (c) tetrahedral intermediate. The charges on the *m*-*tert*-butylphenyl group in *mt*BPA are identical to the charges in the TI. For the reactive sugars with O2 or O3 ionized the charge on the relevant oxygen is −1.15, while all other charges on the glucose unit are unchanged. In methyl glucoside the C4 hydroxyl is a standard one, while the C1 methoxy group has charges of −0.36 and +0.16 on the oxygen and methyl group, respectively.

initio studies,[20] and consistent with a slightly endothermic solution reaction where the gas-phase energetics is modulated by solvation effects (larger solvation energy of the reactants).

All the calculations were carried out with the MD/FEP/EVB program Q.[21] The reacting molecules are placed in the center of a sphere (16 Å radius) of SPC water molecules. The waters are subjected to radial and polarization surface restraints according to a scheme (Marelius and Åqvist, in preparation) inspired by the SCAAS model[22a] and a recent model from Jorgensen.[23] A weak harmonic restraint ($k = 5.0$ kcal mol$^{-1}$ Å$^{-2}$) is applied to keep the centers of methyl glucoside and the cyclodextrin cavity in the vicinity of the water sphere center. Multipole expansion of electrostatic interactions beyond 20 Å was employed for water−water interactions by using the LRF method,[22b] while all other interactions were directly calculated. Water bonds and angles were constrained with the SHAKE procedure.[18c] The MD trajectories were run at a constant temperature of 300 K with a time step of 1 fs.

When calculating the free energy surfaces of reactions 1 and 2 the reverse process of breaking the C−O bond in the tetrahedral intermediates was simulated to attain the most efficient configurational sampling. The mapping potential is then used to generate MD trajectories when the C−O bond is slowly switched off. While this procedure is quite straightforward in the case of reaction with an alkoxide ion of methyl glucoside, the situation with cyclodextrin turned out to be more complicated. We could not start from the gas-phase optimized geometries of the adducts, since they provide unrealistic structures with the substrate molecule moved out of the cavity.[15] So, a protocol was used where the MD calculations started from the relaxed geometries of the inclusion complex [*mt*BPA···$\beta$CD$^-$] and during 2 ps runs the C−O bond was forced to be created by applying an additional geometry restraint for the corresponding interatomic distance. The resulting structures of the TI were relaxed during 15 ps runs. That was then followed by simulation of the breaking of the C−O bond with use of the MD/FEP/EVB approach. Thirty values of $\vec{\lambda}$ were taken in the range between (1,0) and (0,1) and interspaced for optimal sampling efficiency. The calculation at each value of $\vec{\lambda}$ included 1 ps of initial equilibration and 3 ps for data collection. In each case free energy profiles were calculated and averaged for both the "forward" and "backward" reactions. Comparison of the free energies obtained from forward and backward summation together with running several trajectories with different initial conditions gives us an estimate of about ±1.5 kcal/mol for the convergence error of the free energy profiles.

## Results and Discussion.

The reaction of the acyl group of phenyl acetate with a secondary alkoxide ion of $\beta$CD, in principle, can lead to formation of both *R* and *S* stereoisomers of the tetrahedral adduct. All four possible structures corresponding to the stereoisomers of the TI at the C2−O2$^-$ and C3−O3$^-$ reaction sites are considered in our simulations. The O2$^-$ and O3$^-$ alkoxide ions of $\beta$CD differ in terms of orientation of the C−O$^-$ bond with respect to the axis of the cavity where the C2−O2$^-$ bond is more inclined in the direction of the cavity interior than the C3−O3$^-$ bond. For stereochemical reasons it could therefore be expected that formation of the TI with the substrate staying inside the macrocyclic cavity involves less steric strain for the O2 site than for the O3 site, which indeed also seems to be the case. The MD structural relaxation of tetrahedral intermediates at the O2 center provides spatial configurations with the phenyl ring located within the cavity both for *R* and *S* stereoisomers. In the case of reaction at the O3 site, only the *R* isomer of the TI corresponds to that kind of the structure, although the substrate then is considerably more pulled out of the cavity due to the fact that O3 is pointing out from the cavity axis. Structural relaxation of the *S* isomer at O3, on the other hand, leads to complete movement of the *m*-*tert*-butylphenyl group out of the cavity due to a large steric strain. Accordingly the *S* isomer of the TI at O3 is omitted from further consideration.

Reaction curves for the formation of the TI from the O2$^-$ and O3$^-$ alkoxide ions of $\beta$CD, calculated with eqs 6 and 7, are presented along with the calibrated reaction profiles for the corresponding reference reactions in Figures 3 and 4, respectively. The immediate result is that the reaction path leading to the *S* isomer of the TI at O2 in $\beta$CD has an activation barrier $\Delta G^{\ddagger}$ that is lower than the barrier for uncatalyzed reaction ($\Delta G^{\ddagger}_{ref} = 21.8$ kcal/mol) by about 3 kcal/mol (Figure 3). The corresponding value of $\Delta G^0$ is slightly higher (∼1 kcal/mol) than the reference value ($\Delta G^0_{ref} = 5$ kcal/mol). Formation of the *R* isomer at O2 has a barrier that is ∼2 kcal/mol higher than the barrier of uncatalyzed reaction and a reaction free

(19) Guthrie, J. P. *J. Am. Chem. Soc.* **1973**, *95*, 6999.
(20) Pranata, J. *J. Phys. Chem.* **1994**, *98*, 1180.
(21) Åqvist, J. *Q*, Version 2.1; Uppsala University, 1996.
(22) (a) King, G.; Warshel, A. *J. Chem. Phys.* **1989**, *91*, 3647. (b) Lee, F. S.; Warshel, A. *J. Chem. Phys.* **1992**, 97, 3100.
(23) Essex, J. W.; Jorgensen, W. L. *J. Comput. Chem.* **1995**, *16*, 951.

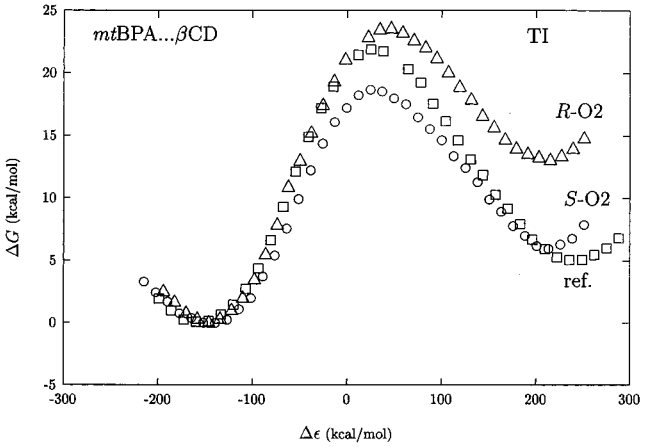


**Figure 3.** Free energy profiles for reactions 1 and 2 at the O2 reaction site of the glucose subunit. The reference reaction in water is denoted by squares while the $\beta$CD-catalyzed *R* and *S* reaction paths are denoted by triangles and circles, respectively.

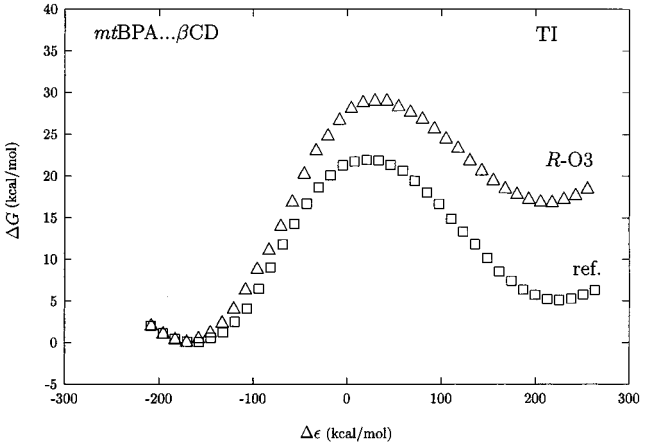


**Figure 4.** Free energy profiles for reactions 1 and 2 at the O3 reaction site of the glucose subunit. The reference reaction in water and the $\beta$CD-catalyzed *R* reaction path are denoted by squares and triangles, respectively.

energy of ~13 kcal/mol (Figure 3). Formation of the *R* isomer at the O3 center has a $\Delta G^{\ddagger}$ value that is about 7 kcal/mol higher than $\Delta G^{\ddagger}_{ref}$ of the reference reaction (Figure 4).

Snapshots of some relevant structures along the reaction pathway leading to formation of the *S* isomer at O2 are presented in Figure 5. It can be noted that the nonpolar part of the substrate resides well inside the cavity both in the inclusion complex and in the TI. In the inclusion complex, the bulky *m-tert*-butyl substituent on the phenyl ring ensures a favorable orientation of the acyl group with respect to the cavity rim with its reactive hydroxyl groups (see also the discussion of steric effects of substituent groups on the hydrolysis rate in refs 8 and 15). In the transition state the acyl group approaches the alkoxide ion while the structure of the macrocycle remains more or less unperturbed (Figure 5b). This is accompanied by an upward movement (cf. Figure 5b) of the phenyl moiety. It can also be noted that the O3 hydroxyl groups of the attacking and preceding sugar residues provide strong hydrogen bonds in the transition state to both the nucleophile and the developing negative charge on the acyl oxygen. The transition state is mainly sampled with the FEP mapping vector $\bar{\lambda}_m = (0.40,0.60)$, and it also corresponds to the average VB state coefficients $c_1^2 = 0.4$ and $c_2^2 = 0.6$, in accordance with the Hammond postulate for an endothermic process. The average C−O bond length at the transition state is found to be 2.0−2.1 Å.

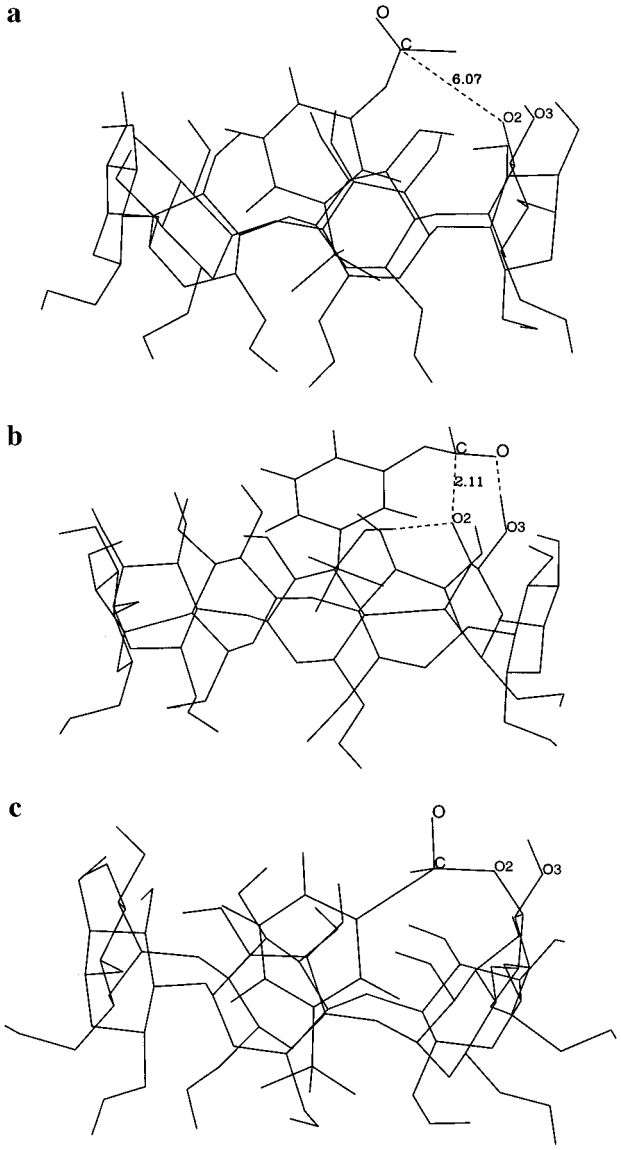


**Figure 5.** Snapshots from the simulations of the $\beta$CD-catalyzed *S* reaction path at O2: (a) inclusion complex, (b) transition state, and (c) tetrahedral intermediate.

In the tetrahedral intermediate the substrate stays deeply located inside the cavity and the glucose subunit of the macrocycle is bent toward the inside of the cavity to adjust to the position of the substrate (Figure 5c). This strain is reflected by a sampling of both chair and skewed conformations of the glucose residue when the TI is approached. Figure 5c shows the TI with the reacting sugar in the skewed conformation that appears to be most stable. The driving force for this distortion of the macrocycle seems to be a strong hydrophobic binding of the substrate, but it can also be noted that the negatively charged acyl oxygen then achieves a maximal exposure to solvent.

The reaction free energy barrier in cyclodextrin differs from that of the uncatalyzed reaction due to contributions coming from solvation and steric energies. Formation of the tetrahedral intermediate in $\beta$CD (cf. Figure 5) is facilitated by the preorganized host (viz. a hydrophobic cavity with OH dipoles on the rim) that allows for a reduction of the desolvation barrier associated with charge delocalization accompanying the approach to the TI. Despite the increased strain of the macrocycle in the TI, it appears that the intermediate is not significantly destabilized relative to the uncatalyzed reaction for the productive pathway leading to the *S* isomer at O2. However, the main

effect is exerted in the transition state where the *S* isomer attains an efficient stabilization by the two O3 hydroxyls adjacent to the reaction center. The binding free energy of the inclusion complex of *mt*BPA with $\beta$CD can be estimated to be about −5.3 kcal/mol,[8a] and the conformational strain of $\beta$CD in the TI is probably of smaller magnitude. Thus, the binding of substrate appears strong enough to keep *mt*BPA in the hydrophobic cavity even in the somewhat strained tetrahedral intermediate. Our calculations also indicate that only formation of the *S* isomer at O2 provides structures where good binding is accompanied by low steric strain. Also very important in this case is that the ionic center remains well exposed to the surrounding water molecules along the entire reaction path (see Figure 5). All other reaction paths correspond to much larger unfavorable steric interactions and also show a more buried character of the negative acyl oxygen in the TI compared to the alkoxide ion of $\beta$CD. Furthermore, in the transition state leading to the *R* isomer at O2 it is evident that only one O3 hydroxyl group (of the preceding residue) can provide strong hydrogen bonding to the two negative oxygens. Our MD/FEP/EVB simulations also explain the problems encountered in the earlier AM1 study[15] where energy minimization failed to locate a low energy reaction path for the TI formation at O2. The AM1/LD calculations of the reaction path for C−O bond cleavage in the TI at O3 formally showed a lowering of the barrier compared to the reaction in water, which was attributed mainly to an electrostatic contribution from the solvation energy. However, these calculations resulted in a structure of the [*mt*BPA···$\beta$CD] complex where the aromatic part of the substrate had moved well out of the cavity and no strong binding to cyclodextrin could exist. This contradicts experimental evidence that catalysis proceeds through the bound state of the substrate. Our present calculations involve extensive molecular dynamics relaxation and thermal sampling of the reactants as the mapping potential successively changes. This is a much more powerful approach than quantum chemical minimization algorithms for exploring the multidimensional potential surfaces with numerous local minima. It is therefore encouraging that catalysis can be obtained with the substrate more or less bound to the host during the entire reaction, as our calculations show, which also appears to be in agreement with experiment. In this case the overall change in reaction barrier (compared to the reference reaction) is determined not only by electrostatic contributions to the solvation energy of the reaction center, but also by the binding energy and steric strain of the macrocycle.

In a force field treatment of the present type, the O2 and O3 sites are not longer identical, and it is most convenient to use two separate reference reactions for these sites when calibrating the EVB potential. This is due to the presence of some (almost) constant nonbonded intramolecular energy contributions that arise from the fixed covalent structure since 1−3 neighbors are excluded from the nonbonded interactions in most FF's (and are instead taken care of by the angle terms). So, the ground-state free energy curves for the reference reactions at both sites are fitted separately to the experimental estimates of $\Delta G^0_{ref}$ and $\Delta G^{\ddagger}_{ref}$. The EVB calibration parameters are thus found to be different in these cases (Table 1), which only reflects the difference in colvalent structure around the two centers. Thus, the present treatment does not address the question of relative reactivity of hydroxyl groups in glucose derivatives, but it is directly applicable to comparison of the reactivity of equivalent centers in methyl glucoside and in $\beta$CD. Of course, the question of stereoselectivity in hydrolysis by $\beta$CD is of considerable interest and the calculated free energy profiles show that the only favorable channel of hydrolysis in $\beta$CD is associated with the formation of the *S* stereoisomer of the TI at O2. Figures 3 and 4, however, do not provide direct information about the energy of this route relative to the uncatalyzed reaction at O3 of methyl glucoside, which may be important for discussing the stereoselectivity of hydrolysis in $\beta$CD.

Some insight regarding reactivity of the secondary hydroxyl groups of $\beta$CD can be obtained from their p$K_a$ values. The corresponding estimates for the reactive −OH groups in methyl glucoside using the empirical scheme from ref 24 indicate that the p$K_a$ of the secondary hydroxyl group at C2 (12.7 units) is 0.5 units lower than the p$K_a$ of the C3 hydroxyl group (13.2 units). The earlier AM1/LD calculations[15] of $\beta$CD anions in a polar environment also predicted greater stability of the $O2^-$ anion compared to $O3^-$. The secondary hydroxyl groups of cycloamyloses are, besides hydrolysis, involved in reactions of methylation by diazomethane in the presence of base.[25] The data from ref 25 suggest that the C3 hydroxyl group is the reactive center for methylation. Furthermore, the methylated cyclodextrin (dodecamethylcyclohexaamylose) is inactive in hydrolysis but, in view of our study, the methylation data do not provide enough evidence in favor of the C3 hydroxyls as the hydrolytic reaction site. While the O3-methylated macrocycle certainly cannot be reactive at the O3 site, the reaction at O2 would also be impeded due to steric hindrance at the reaction site as well as a higher p$K_a$ resulting from the additional nearby methyl group. Particularly, the *S* isomer of the transition state as well as the TI would be destabilized due to unfavorable steric and electrostatic interactions between the O3 methyl group and the negative acyl oxygen. In this manner methylation at O3 could also well be inhibitory for reaction at O2. Thus, taken together the bulk of existing data is entirely consistent with our conclusion that the reactive site in $\beta$CD is of the $O2^-$ type.

## Conclusions

In this work we have performed a molecular dynamics FEP/EVB study of the rate-limiting step in the biomimetic hydrolysis of phenyl ester catalyzed by cyclodextrin in solution. For the reaction of *m-tert*-butylphenyl acetate in $\beta$-cyclodextrin four possible reactive channels are considered. Only one favorable reaction route leading to formation of the *S* stereoisomer of the tetrahedral intermediate at the C2 hydroxyl site is found. The calculated activation free energy barrier of $\Delta G^{\ddagger} \approx 18.7$ kcal/mol is in excellent agreement with the experimentally estimated value of $\Delta G^{\ddagger} \approx 18.6$ kcal/mol for this reaction. An important result of the simulations is that the substrate stays more or less bound to the macrocycle during the entire reaction. This is in complete agreement with existing experimental data on the role of substrate binding and competetive inhibition in hydrolysis by cyclodextrins.[8] Earlier quantum chemical AM1/LD calculations[15] of the reaction enthalpies in solution demonstrated that the lowering of the activation barrier in cyclodextrin could in principle be explained by the electrostatic effect of the nonpolar macrocycle cavity. The role of substrate binding was, however, completely missing from those calculations where, in fact, the transition states and the tetrahedral intermediates corresponded to the situation with the substrate moved well out of the cavity. Our present calculations provide a more complicated and, in most respects, more realistic picture of the structural changes along the reaction path. The macrocycle adjusts its structure

(24) Perrin, D. D.; Dempsey, B.; Serjeant, E. P. *p$K_a$ Prediction for Organic Acids and Bases*; Chapman & Hall: London, 1981.

(25) Staerk, J.; Schlenk, H. In *Abstracts, 149 National Meeting of the American Chemical Society*, Detroit, MI; American Chemical Society: Washington, DC, 1965; p 11C.

after the C−O chemical bond has started to form and, while the substrate moves partly out in the transition state, it can be accommodated as the tetrahedral intermediate is approached by a slight distortion of the macrocycle. The reaction barrier in cyclodextrin is determined by contributions coming from electronic interactions at the reaction center, changes in solvation energies, binding energy, and structural strain of the macrocycle. In particular, we find that the transition state leading to the *S* isomer of the O2 adduct can be efficiently stabilized by the O3 hydroxyls adjacent to the reaction center, while still retaining a high degree of solvent exposure.

**Acknowledgment.** We gratefully acknowledge support for this work from the Faculty of Science and Technology at Uppsala University. V.L. is most thankful to Prof. Carol Venanzi for initiating his interests in cyclodextrins. J.Å. also acknowledges support from the E.C. Biotechnology program (DGXII) and from the NFR.

JA973799W